



Pharmacokinetic optimisation of novel indole-2-carboxamide cannabinoid CB₁ antagonists

Phillip M. Cowley^{a,*}, James Baker^c, Kirsteen I. Buchanan^a, Ian Carlyle^a, John K. Clark^a, Thomas R. Clarkson^a, Maureen Deehan^b, Darren Edwards^a, Yasuko Kiyoi^a, Iain Martin^c, Dawn Osbourn^c, Glenn Walker^b, Nick Ward^c, Grant Wishart^a

^a Department of Chemistry, MSD, Newhouse, Lanarkshire ML1 5SH, UK

^b Department of Molecular Pharmacology, MSD, Newhouse, Lanarkshire ML1 5SH, UK

^c Department of Pharmacology, MSD, Newhouse, Lanarkshire ML1 5SH, UK

ARTICLE INFO

Article history:

Received 17 December 2010

Revised 2 February 2011

Accepted 3 February 2011

Available online 19 February 2011

Keywords:

Cannabinoid

CB₁

Antagonist

Indole

Pharmacokinetics

CYP3A4

Glucuronidation

ABSTRACT

The pharmacokinetic based optimisation of a novel series of indole-2-carboxamide antagonists of the cannabinoid CB₁ receptor is disclosed. Compound **24** was found to be a highly potent and selective cannabinoid CB₁ antagonist with high predicted human oral bioavailability.

© 2011 Elsevier Ltd. All rights reserved.

The identification of cannabinoid CB₁ and CB₂ receptors and their endogenous ligands in the early 1990s provided further encouragement to the research community to identify novel ligands for these G-protein coupled receptors.¹ In particular, the discovery of rimonabant (SR141716A, **1**) provided an important tool with which to probe the therapeutic potential of selective cannabinoid CB₁ receptor antagonists.² Indeed, this compound was approved for use in the treatment of obesity in Europe and other territories. Subsequently, psychiatric adverse events were noted in clinical use and the product was withdrawn from the market.

We have previously described an optimisation programme leading to the discovery of novel cannabinoid CB₁ receptor antagonists **2** and **3** (Fig. 1).³ Compound **3**, in particular, was noted to be a potent antagonist both in vitro and in vivo and was subsequently the subject of further studies. During this further profiling, compound **3** was shown to undergo metabolism by both oxidation (mediated by CYP3A4) and direct glucuronidation (Fig. 2). Rat hepatic portal vein cannulation studies showed that both metabolites were found in plasma from the hepatic portal vein following an oral dose of **3** (data not shown). This suggested that gut wall

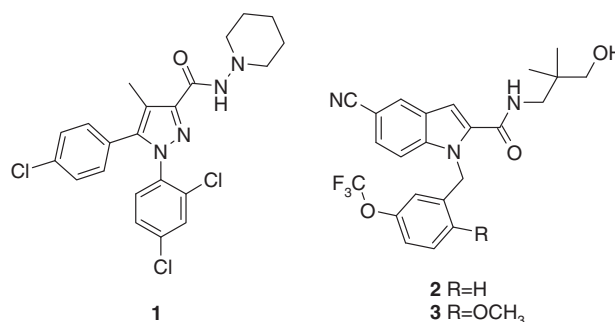


Figure 1. Structures of rimonabant (**1**), **2** and **3**.

* Corresponding author.

E-mail address: phillip.cowley@tppgd.com (P.M. Cowley).

metabolism by both P450 and UGT mechanisms, in addition to hepatic metabolism, may limit oral bioavailability. The rate of metabolism by CYP3A4 was measured for several 5-chloro and 5-cyano indole-2-carboxamides.⁴ For the 5-cyano indole-2-carboxamide subseries a convincing relationship between the rate of CYP3A4 metabolism and $c \log P^5$ was identified (Fig. 3). Medicinal chemistry design strategies were employed to reduce the rate of metabolism by balancing the lipophilicity of the series with the potential

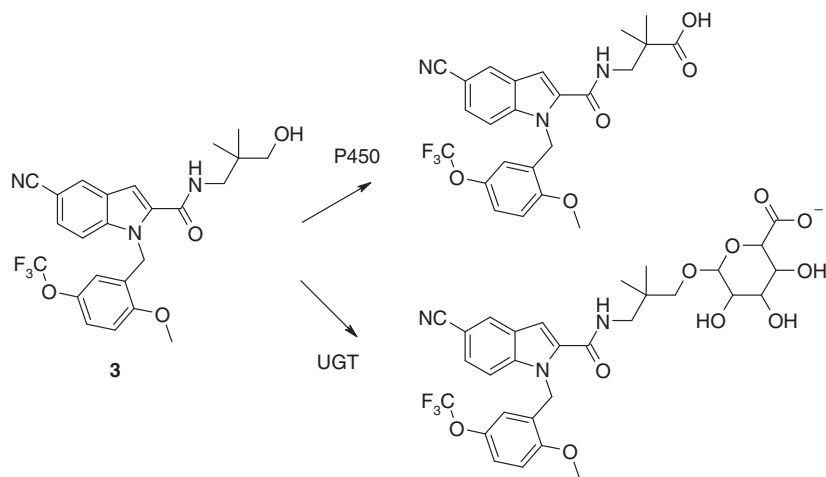


Figure 2. Metabolism of compound **3** in rat hepatocytes.

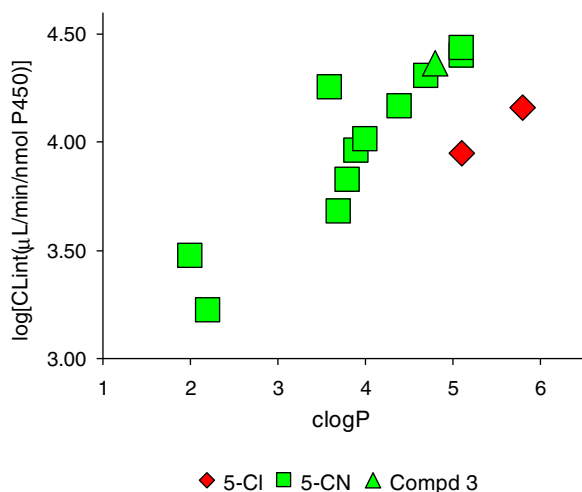


Figure 3. Plot of rate of CYP3A4 metabolism versus $c \log P$ for selected compounds from the indole-2-carboxamide series of CB₁ antagonists.

for blocking sites of metabolism. Compounds were ranked by in vitro assessment of both intestinal and hepatic P450 and UGT stability. The aim was to identify compounds with improved predicted human pharmacokinetics compared to **3** and to gain confidence in these predictions with data across pre-clinical species.

The in vitro to in vivo extrapolation (IVIVE) of clearance by glucuronidation was known to be challenging, largely due to differences in experimental set-up influencing the rate of in vitro glucuronidation, for example, the inhibitory effects of fatty acids and enabling of compound access with alamethicin.^{6–8} To increase confidence in IVIVE for a combined P450/UGT model⁹ (Fig. 4) incorporating intestinal and hepatic metabolism, predictions for **3** and raloxifene (Evista, known to undergo extensive gut first pass metabolism^{10,11}) in a range of species were compared with in-house pre-clinical and published clinical PK data. Subsequent to these studies, alternative models for prediction of gut extraction from in vitro data have been suggested in the literature, particularly for compounds metabolised predominantly by CYP3A4.^{12–14}

As demonstrated in Table 1, the combined UGT/P450 approach predicted clearance and oral bioavailability with reasonable accuracy, suggesting that ranking compounds on the basis of such in vitro stability data may be a useful approach. Interestingly, raloxifene was shown to undergo both direct glucuronidation

and NADPH-mediated oxidation, complementing previous reports of raloxifene interactions with CYP3A4.¹⁵ Compound **3** showed marked species differences in extent of P450 and UGT mediated metabolism, with these species differences being reflected in the in vivo PK data.

Compounds from the indole-2-carboxamide series were assessed for potency as antagonists of the human CB₁ receptor in a CB₁ reporter gene assay as described previously.¹⁶ The values of pIC₅₀ are reported as the means of at least two independent experiments. Compounds were subsequently selected for screening in human microsomes from gut and liver, primed for both P450 and UGT pathways to provide an approximate ranking with respect to predicted PK profile.

The synthesis of indole-2-carboxamide analogues of compound **3** is depicted in Scheme 1, all starting materials and reagents were purchased from commercial sources unless otherwise stated. Ethyl 5-cyanoindole-2-carboxylate (**4**) was benzylated by deprotonation with sodium hydride followed by addition of the appropriate benzyl bromide to afford **5**. Hydrolysis gave the acid (**6**), which was converted to the amides (**7–31**) by coupling with the amine using 1-hydroxybenzotriazole (HOBt) and 1-ethyl-3-[3-dimethylamino-propyl]carbodiimide] hydrochloride (EDCI).

Synthesis of non-commercially available amines is described in Scheme 2. 4-Amino-1,1,1-trifluoro-2-trifluoromethylbutan-2-ol (**34**) was obtained from the reaction of the bis(trifluoromethyl)butyrate (**32**) in aqueous ammonia, followed by reduction of the amide (**33**) with lithium aluminium hydride in tetrahydrofuran. 1-(1-(Aminomethyl)cyclopentyl)ethanol (**38**) was prepared from ethyl cyanoacetate (**35**) treated with sodium ethoxide and 1,4-dibromobutane to give ethyl 1-cyanocyclopentanecarboxylate (**36**) which on treatment with (trimethylsilyl)methyl lithium followed by addition of water gave 1-acetylpentanecarbonitrile (**37**). Reduction with lithium aluminium hydride afforded the desired 1-(1-(aminomethyl) cyclopentyl)ethanol (**38**). 1-(2-Aminoethyl)cyclobutanol (**41**) was obtained from treating acetonitrile with lithium diisopropylamide at $-70\text{ }^{\circ}\text{C}$ then addition of cyclobutanone (**39**), the resulting cyano alcohol (**40**) was hydrogenated in the presence of Raney nickel. Where the benzyl bromides were not commercially available they were prepared from the appropriate benzyl alcohol using PPh₃ and CBr₄.

From our earlier SAR exploration of this indole-2-carboxamide series it was clear that the indole N-1 benzyl moiety is tolerant to multiple substituents at the *ortho* and *meta* positions, although there was a general preference for more lipophilic substituents.³ In a first attempt to lower metabolic clearance whilst maintaining

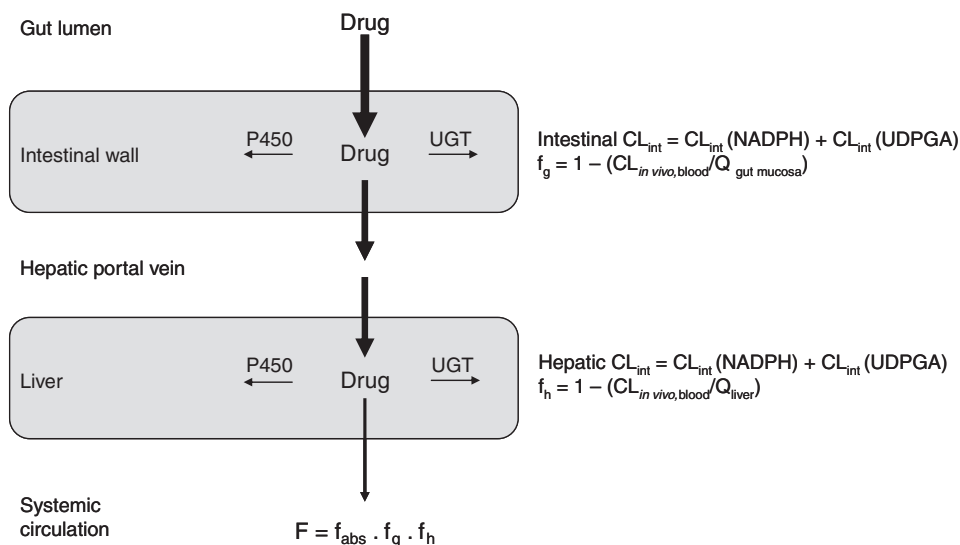


Figure 4. Model for predicting gut and intestinal metabolism.

Table 1
Intrinsic clearances, predicted and observed pharmacokinetic data for raloxifene and **3** in a range of species

Compd	Species	CL _{int} (μL/min/mg)				CL _{pred} (mL/min/kg)	F _{pred} (%)	CL _{obs} (mL/min/kg)	F _{obs} (%)
		Gut		Liver					
		NADPH	UGT	NADPH	UGT				
Raloxifene	Mouse	0	34	66	0	69	15	108	10
	Rat	0	5	79	11	55	21	58	4
	Dog	0	22	178	26	23	17	40	5
	Human	0	346	79	24	18	5	21	2
3	Mouse	0	0	45	0	60	9	17	30
	Rat	0	0	69	191	72	6	104	8
	Dog	0	0	0	7	7	68	7	67
	Human	0	68	69	31	19	4	—	—

CL_{int}—in vitro intrinsic clearance (values of 0 indicate <6 μL/min/mg).

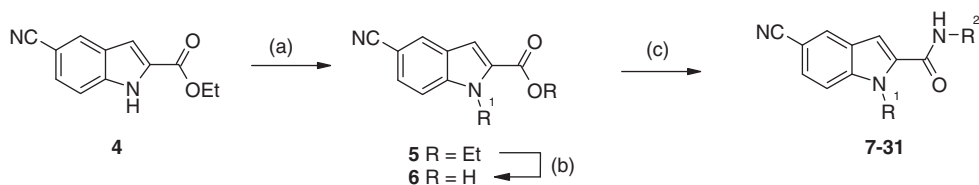
CL_{pred}—predicted in vivo plasma clearance.

CL_{obs}—observed in vivo plasma clearance.

F_{pred}—predicted oral bioavailability.

F_{obs}—observed oral bioavailability.

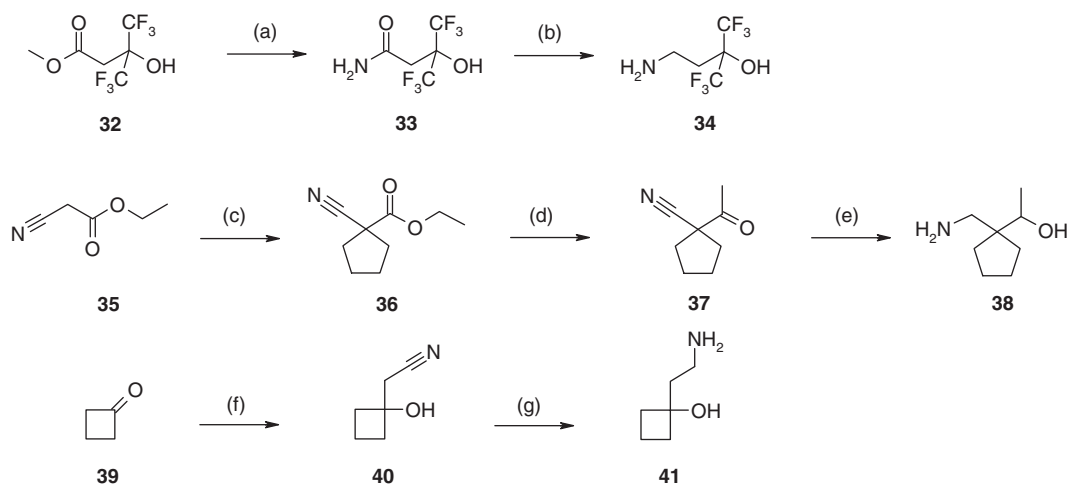
See Ref. 9 for details of the assays.



Scheme 1. Reagents and conditions: (a) R¹Br, NaH, DMF, 60 °C; (b) KOH, EtOH/H₂O, 60 °C; (c) R²NH₂, EDCI, HOBT, Et₃N, CH₂Cl₂, rt.

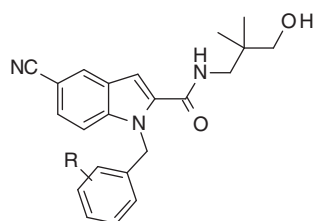
potency, subtle changes to substituents and lipophilicity in the benzyl region were pursued (Table 2). 2-Ethoxy-5-trifluoromethoxy benzyl analogue **7** showed a seven-fold decrease in CB₁ antagonist potency compared to compound **3** with no improvement in intrinsic clearance. 3,5-Dichloro analogue **8** was also disappointing showing a modest 4.5-fold decrease in CB₁ potency and high intrinsic clearance. Compounds **9–15** (c log *P* range 4.06–4.81), exhibited similar or reduced lipophilicity to compound **3** (c log *P* = 4.76) and all showed high CB₁ antagonist potency. However, intrinsic clearance again showed no improvement. It was evident that subtle changes to the benzyl region were failing to decrease hepatic and gut wall metabolism, therefore, combinations

of modifications to the amide and benzyl moieties were explored (Table 3). Cycloalkyl derivatives **16–20** showed similar or decreased CB₁ potency compared to **3**, however no significant improvement in metabolic stability was achieved. Adopting a more direct approach by blocking the major site of P450 metabolism via substitution of the carbon adjacent to the hydroxyl moiety resulted in significant success. Chain shortened tertiary alcohols **21** and **22** showed significantly reduced glucuronidation and P450 mediated metabolism upon comparison with **3**, this was accompanied with an order of magnitude decrease in CB₁ receptor potency. 3-Hydroxy-3-methylbutyl analogue **23** showed a similar profile to **21** and **22**. However, CB₁ potency could be partially recovered via changes



Scheme 2. Reagents and conditions: (a) NH_4OH , MeOH , rt, 40 h; (b) LiAlH_4 , THF , 0°C , 20 h; (c) $\text{Br}(\text{CH}_2)_4\text{Br}$, NaOEt , EtOH , 70°C , 4 h; (d) TMSCH_2Li , pentane, MeOH , 0°C , 35 h; (e) LiAlH_4 , THF , rt, 18 h; (f) MeCN , LDA , THF , -70°C , 2 h; (g) Raney Nickel, H_2 , EtOH , 5 bar, 50°C , 20 h.

Table 2
Benzyl substituent SAR



Compd	R	CB ₁ pIC ₅₀	Gut CL _{int} (NADPH)	Gut CL _{int} (UGT)	Liver CL _{int} (NADPH)	Liver CL _{int} (UGT)
1	H	7.95	0	0	69	0
2	3-OCF ₃	8.74	0	136	62	20
3	2-OCH ₃ , 5-OCF ₃	8.93	0	68	69	31
7	2-OCH ₂ CH ₃ , 5-OCF ₃	8.08	0	103	103	20
8	3-Cl, 5-Cl	8.27	0	98	103	22
9	2-OCH ₃ , 5-Cl	8.70	0	63	83	10
10	2-OCH ₃ , 5-Br	9.11	0	94	104	23
11	2-OCH ₃ , 5-CH ₃	9.12	0	64	191	23
12	2-CH ₃ , 5-CF ₃	9.29	0	102	180	16
13	2-CH ₃ , 5-Cl	9.24	0	124	119	23
14	2-CH ₃ , 5-CH ₃	9.20	0	124	257	29
15	3-OCH ₂ CH ₂ CH ₃	8.81	13	45	156	10

CL_{int} in $\mu\text{L}/\text{min}/\text{mg}$ (from duplicate assays with human microsomes)

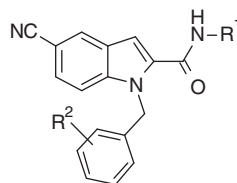
in the benzyl moiety. Combination of the 3-hydroxy-3-methylbutyl amide with a 2-methyl-5-trifluoromethyl substituted benzyl resulted in compound **24** showing only a four-fold decrease in potency compared to **3**, yet maintaining the promising in vitro metabolic profile of analogues **21–23**. Secondary alcohols **25** and **26** maintained high CB₁ receptor potency, however P450 mediated hepatic metabolism was significantly increased upon comparison with the tertiary alcohols. Analogue **27** exhibited a reasonable profile and high potency but cyclobutyl alcohols **28** and **29** together with primary alcohol **30** showed hepatic P450 intrinsic clearances in the same range as for compound **3**. Highly lipophilic secondary alcohol **31** unsurprisingly showed high intrinsic clearances.

Selected compounds with good predicted PK and high CB₁ receptor potency were advanced to in vivo evaluation in a reversal of mouse hypothermia induced by the cannabinoid agonist WIN 55,212-2 (Table 4).¹⁷ Compound **24** dosed orally showed potent reversal of WIN 55,212-2 induced hypothermia comparable to that of rimonabant (**1**) and the previously disclosed **3** (ID₅₀s **24** = 1.16,

rimonabant (**1**) = 1.29, **3** = 0.88 $\mu\text{mol}/\text{kg}$). Compound **23** (ID₅₀ = 9.67 $\mu\text{mol}/\text{kg}$) was less potent and compounds **21** and **22** (both with ID₅₀ > 10 $\mu\text{mol}/\text{kg}$) were inactive at the doses tested. The affinities of compounds at the cannabinoid receptors were determined by radioligand binding experiments performed at least in duplicate. Affinity for CB₁ was measured by competition with [³H]SR141716A binding to membranes prepared from CHO cells expressing the human CB₁ receptor. Affinity for CB₂ was measured by competition with [³H]CP55,940 binding to recombinant human CB₂ receptors expressed in Sf9 cell membranes. Compounds **21–24** all showed high CB₁ receptor affinity. CB₂ receptor affinity was only measured for **24** which was found to be greater than 1000-fold selective for the CB₁ receptor versus the CB₂ receptor.

The human microsomal stability screening identified **24** as having a potentially superior PK profile than **3**. As shown in Table 5, the same in vitro models predicted in vivo PK reasonably well across species and, most importantly, suggested that **24** should have a much improved human PK profile. In human liver micro-

Table 3
Benzyl and amide substituent SAR



Compd	R ¹	R ²	CB ₁ pIC ₅₀	Gut CL _{int} (NADPH)	Gut CL _{int} (UGT)	Liver CL _{int} (NADPH)	Liver CL _{int} (UGT)
16	*	2-OCH ₃ , 5-OCF ₃	8.29	0	51	139	18
17	*	2-OCH ₃ , 5-CF ₃	8.88	0	49	155	7
18	*	2-OCH ₃ , 5- <i>t</i> Bu	8.83	0	26	188	0
19	*	2-OCH ₃ , 5-Cl	8.59	0	179	196	34
20	*	2-CH ₃ , 5-F	8.31	0	175	190	49
21	*	2-OCH ₃ , 5-OCF ₃	7.65	0	8	0	0
22	*	2-OCH ₃ , 5-CF ₃	7.94	0	0	7	0
23	*	3-OCF ₃	7.87	0	9	9	0
24	*	2-CH ₃ , 5-CF ₃	8.29	0	0	12	0
25	*	3-OCF ₃	8.05	0	0	113	0
26	*	3-OCF ₃	8.09	26	0	59	31
27	*	3-OCF ₃	8.22	0	0	20	24
28	*	2-OCH ₃ , 5-CF ₃	8.83	0	0	88	0
29	*	3-OCF ₃	8.58	0	0	78	0
30	*	2-OCH ₃ , 5-Br	8.03	0	0	41	0
31	*	3-OCF ₃	8.29	99	0	505	9

CL_{int} in μL/min/mg (from duplicate assays with human microsomes).

Table 4
Reversal of WIN 55,212-2 induced hypothermia

Compd	Hypothermia ID ₅₀ μmol/kg (95% CI)	CB ₁ pK _i	CB ₂ pK _i
1	1.29 (0.40–4.17)	9.03	6.07
2	3.42 (0.97–12.04)	9.10	<5.0
3	0.88 (0.58–1.34)	9.40	<5.0
21	>10	8.26	ND
22	>10	8.12	ND
23	9.67 (2.91–32.10)	8.30	ND
24	1.16 (0.23–5.93)	8.36	<5.0

ND = not determined.
CI = confidence interval.
ID = inhibitory dose.

some oxidation was observed at three distinct sites on the molecule, demonstrating that metabolism no longer occurred at the alcohol. In wider selectivity profiling **24** showed no appreciable affinity (estimated pK_i <5) at 10 μM for a panel of 63 molecular targets comprising of GPCRs, ion channels, transporters, enzymes and nuclear receptors.

In summary, a pharmacokinetic based optimisation utilising in vitro assays to assess tissue and species specific intrinsic clearances has been employed. Compound **24**¹⁸ has been identified as a novel potent and selective CB₁ antagonist. Furthermore, **24** showed reduced human intrinsic clearance compared to starting point **3**, leading to a significantly increased predicted human oral bioavailability. The compound displayed reversal of the hypothermia induced by a cannabinoid agonist in vivo, with potency comparable to that of rimonabant.

Table 5
Intrinsic clearances, predicted and observed pharmacokinetic data for **24** in a range of species

Compd	Species	CL _{int} (μL/min/mg)				CL _{pred} (mL/min/kg)	F _{pred} (%)	CL _{obs} (mL/min/kg)	F _{obs} (%)
		Gut		Liver					
		NADPH	UGT	NADPH	UGT				
24	Mouse	0	0	33	0	53	14	10	31
	Rat	0	0	>280	>280	> 78	< 8	200	2
	Dog	0	0	17	0	14	52	15	42
	Human	0	0	12	0	7	65	–	–

Acknowledgements

We thank our Analytical Chemistry colleagues for structure and purity determination.

References and notes

- Howlett, A. C.; Barth, F.; Bonner, T. I.; Cabral, G.; Casellas, P.; Devane, W. A.; Felder, C. C.; Herkenham, M.; Mackie, K.; Martin, B. R.; Mechoulam, R.; Pertwee, R. G. *Pharmacol. Rev.* **2002**, *54*, 161.
- Rinaldi-Carmona, M.; Barth, F.; Héaulme, M.; Shire, D.; Calandra, B.; Congy, C.; Martinez, S.; Maruani, J.; Néliat, G.; Caput, D.; Ferrara, P.; Soubrié, P.; Brelière, J. C.; Le Fur, G. *FEBS Lett.* **1994**, *350*, 240.
- Cowley, P. M.; Baker, J.; Barn, D. R.; Buchanan, K. I.; Carlyle, I.; Clark, J. K.; Clarkson, T. R.; Deehan, M.; Edwards, D.; Goodwin, R. R.; Jaap, D.; Kiyoi, Y.; Mort, C.; Palin, R.; Prosser, A.; Walker, G.; Ward, N.; Wishart, G.; Young, T. *Bioorg. Med. Chem. Lett.* **2011**, *21*, 497.
- Compounds were incubated at 1 μM with human recombinant CYP3A4 (50 pmol/mL, BD Biosciences) and 1 mM NADPH. Compound loss was measured in duplicate time-course assays with detection using LC–MS/MS.
- Log P values were calculated using *c log P* 4.3, BioByte Corp. 201 W. 4th St. #204 Claremont, CA 91711-4707, USA.
- Fisher, M. B.; Paine, M. F.; Strelevitz, T. J.; Wrighton, S. A. *Drug Metab. Rev.* **2001**, *33*, 273.
- Miners, J. O.; Smith, P. A.; Sorich, M. J.; McKinnon, R. A.; MacKenzie, P. I. *Annu. Rev. Pharmacol. Toxicol.* **2004**, *44*, 1.
- Tsoutsikos, P.; Miners, J. O.; Stapleton, A.; Thomas, A.; Sallustio, B. C.; Knights, K. M. *Biochem. Pharmacol.* **2004**, *67*, 191.
- Non-restricted well stirred model using intrinsic clearance data from the sum of NADPH and UDPGA dependent pathways. Duplicate microsomal incubations (hepatic microsomes prepared in-house for pre-clinical species, BD Biosciences for human; small intestinal microsomes all from BioPredic (TCS Cellworks, UK)) were performed with 0.5 mg protein/mL at 1 μM drug concentration supplemented with either 1 mM NADPH at pH 7.4 (P450 assay) or 2 mM UDPGA, 50 μg/mL alamethicin, 1 mM MgCl₂ at pH 7.1 (UGT assay). The following physiological parameters were used for prediction of human PK: hepatic blood flow (Q_h) 21 mL/min/kg, liver weight 21 g/kg, liver microsomal protein 45 mg/g, intestinal mucosal blood flow 4.6 mL/min/kg, intestine weight 30 g/kg, intestinal microsomal protein 3 mg/g. Estimates of fraction absorbed (F_{abs}) were ≥38% for compound **3** (rat HPV data), 100% for compound **24** (rat HPV data) and 60% for raloxifene (Ref. 11).
- Kemp, D. C.; Fan, P. W.; Stevens, J. C. *Drug Metab. Dispos.* **2002**, *30*, 694.
- Hochner-Celnikier, D. *Eur. J. Obstet. Gynecol. Reprod. Biol.* **1999**, *85*, 23.
- Yang, J.; Jamei, M.; Rowland, Y. K.; Tucker, G. T.; Rostami-Hodjegan, A. *Curr. Drug Metab.* **2007**, *8*, 676.
- Gertz, M.; Harrison, A.; Houston, J. B.; Galetin, A. *Drug Metab. Dispos.* **2010**, *38*, 1147.
- Kadono, K.; Akabane, T.; Tabata, K.; Gato, K.; Terashita, S.; Teramura, T. *Drug Metab. Dispos.* **2010**, *38*, 1230.
- Chen, Q.; Ngui, J. S.; Doss, G. A.; Wang, R. W.; Cai, X.; DiNinno, F. P.; Blizzard, T. A.; Hammond, M. L.; Stearns, R. A.; Evans, D. C.; Baillie, T. A.; Tang, W. *Chem. Res. Toxicol.* **2002**, *15*, 907.
- Price, M. R.; Baillie, G. L.; Thomas, A.; Stevenson, L. A.; Easson, M.; Goodwin, R.; McLean, A.; McIntosh, L.; Goodwin, G.; Walker, G.; Westwood, P.; Marrs, J.; Thomson, F.; Cowley, P.; Christopoulos, A.; Pertwee, R. G.; Ross, R. A. *Mol. Pharmacol.* **2005**, *68*, 1484.
- The antagonist or vehicle (5% mulgofen in saline, 10 mL/kg) was administered p.o. 75 min before rectal temperature was measured. WIN 55,212-2 mesylate (10 μmol/kg, 10 mL/kg) was administered sc 60 min prior to the rectal temperature measurement. The 60 min pre-treatment with WIN 55,212-2 mesylate corresponded to the maximal hypothermia attained by this agonist. Rectal temperature was measured using a metal probe with a Fluke 51 K/J thermometer. The probe was covered in a lubricant (vaseline) and was inserted approximately 1.5 cm into the rectum. The highest temperature stable for 10 s was recorded. Following completion of the test animals were humanely terminated.
- Analytical data for compound 24*: ESI-MS: *m/z* = 444.3 [M+H]⁺, 426.0 [M–OH]⁺. ¹H NMR (400 MHz, CDCl₃) δ: 8.03–8.05 (d, *J* = 1.6 Hz, 1H), 7.49 (dd, *J* = 1.5 and 8.7 Hz, 1H), 7.45 (broad, 1H), 7.41–7.44 (dd, *J* = 1.2 and 8.0 Hz, 1H), 7.38 (d, *J* = 1.2 and 8.0 Hz, 1H), 7.30 (d, *J* = 7.8 Hz, 1H), 7.22 (dd, *J* = 1.5 and 8.7 Hz, 1H), 7.00 (s, 1H), 6.47 (s, 1H), 5.87 (s, 2H), 3.50–3.57 (m, 2H), 2.47 (s, 3H), 1.72 (m, 2H), 1.30 (s, 6H).